RECENT UPGRADE OF ECRH SYSTEM AND RESULTS OF THE HIGH POWER LONG PULSE INJECTION IN THE LHD

S. Kubo[1], *T. Shimozuma*[1], *Y. Yoshimura*[1],*S. Inagaki*[1], *T. Notake*[2], *H. Idei*,[3], *K. Ohkubo*[1], *R. Kumazawa*[1], *Y. Nakamura*[1], *K. Saito*[1],*T. Seki*[1], *T. Mutoh*[1], *Y. Takita*[1], *S. Kobayashi*[1], *S. Ito*[1], *Y . Mizuno*[1], *F. Gandini*[4], *I. Kazanski*[5], *A. Kruglov*[5], *V. Kurbatov*[5], *E. Tai*[5] *and LHD experimental group*[1]

[1]National Institute for Fusion Science, Toki, Gifu 509-5292, Japan
[2]Dept. of Energy Engineering and Science, Nagoya Univ., Nagoya, 464-8603, Japan
[3]Advanced Fusion Research Center, Research Institute for Applied Mechanics, Kyushu University, Kasuga, 816-8580, Japan
[4]CNR, Instituto di Fisica del Plasma, via Cozzi 53, 20125 Milano, Italy
[5]GYCOM, Ulyanov str. 46, 603950 Nizhny Novgorod, Russia

e-mail: kubo@LHD.nifs.ac.jp

One of the main objectives of the Large Helical Device is to extend the plasma confinement database for helical systems and to demonstrate such extended plasma confinement properties to be sustained in steady state. Electron cyclotron resonance heating (ECRH) plasmas have been extensively used for these confinement study of the LHD experiment from the initial operation of the LHD. The ECRH system is upgraded step by step to inject the power more than 2 MW in LHD. Various optimizations of the injection condition are performed simultaneously. As the result of this power increase and the optimization of the injection condition, central electron temperature of more than 10 keV is achieved near the magnetic axis. The electron temperature profile is characterized by a steep gradient similar to those of an internal transport barrier observed in tokamaks and stellarators. Another important objective of LHD is to demonstrate CW plasma sustainment. Injection of 70 kW power for 766 sec is performed with using CW gyrotron. The plasma with averaged density of less than 1×10^{18} m^{-3} and averaged ECE radiation temperature of 240 eV is sustained for 756 sec without radiation collapse.

Introduction

One of the main objectives of the Large Helical Device is to extend the plasma confinement database for helical systems and to demonstrate such extended plasma confinement properties to be sustained in steady state [1,2]. Electron cyclotron resonance heating (ECRH) plasma have been extensively used for these confinement study of the LHD experiment from the initial operation of the LHD.

Recently, the ECRH system is upgraded to operate four 168 GHz, two 84 GHz, and two 82.7 GHz gyrotrons, simultaneously. A 84GHz CPD diode CW gyrotron

with diamond window is also operated to perform long pulse discharge. One of the evacuated lines is shared for long pulse injection.

Various system optimizations have been done for the ECRH system. Improving the coupling efficiencies of the output from gyrotron to the waveguide had been critical to prevent the arcing inside the waveguide. The antenna system had been designed so as to realize narrow local power deposition profile. Optimization of the heating position in accordance with the target plasma condition have been done by adjusting the injection angle. Sensitive adjustment of the injection angle and polarization is required in particular for the heliotron torsatron type magnetic configuration, because of its complex resonance surface structures and magnetic shear.

As the result of these optimizations, central electron temperature of more than 10 keV with the electron density of 0.6×10^{19} m^{-3} is achieved near the magnetic axis [3]. The electron temperature profile is characterized by a steep gradient similar to those of an internal transport barrier observed in tokamaks and stellarators. The extension of the plasma parameter in such low collisional regime accelerated the study on the structure formation of the electron temperature and its relation to the radial electric field expected from neoclassical transport theory and resultant internal transport barrier in the LHD [4]. One of the proposed mechanisms of this improvement is the suppression of the turbulent transport by velocity or radial electric field shear. Attaining high electron temperature itself is the result of the improvement of the confinement but also open the way to investigate the improved confinement mechanism in the collisionless regime. Achievement of relatively high electron temperatures has been reported from mid scale stellarators as CHS [5], and various explanations have been given for the improved energy confinement. Since the LHD has a higher aspect ratio than the CHS, the LHD has a better orbit of trapped particles, and as the magnetic axis is shifted inward it approaches advanced helical systems in the properties of its drift orbits. Thus, the LHD plays a unique role in understanding the mechanism of the ITB in terms of space potential.

The continuous or the long pulse sustainment of the plasma is another important missions for the LHD, since the confining magnetic field is produced by external super conducting coils. The ECRH system is upgraded to demonstrate the continuous plasma sustainment in LHD. This upgrade includes setting and operation of 84 GHz CW gyrotron, the enforcement of the cooling system along the waveguide transmission line, and installation of an mirror less antenna system. Injection of about 70 kW demonstrated that the plasma with the averaged density of 2.4×10^{17} m^{-3} could be sustained for more than 750 sec.

Electron Cyclotron Heating System in LHD

Bird eye's view of ECH system in LHD operated during last experimental campaign is shown in Fig. 1. In order to provide the high voltage to the gyrotrons,

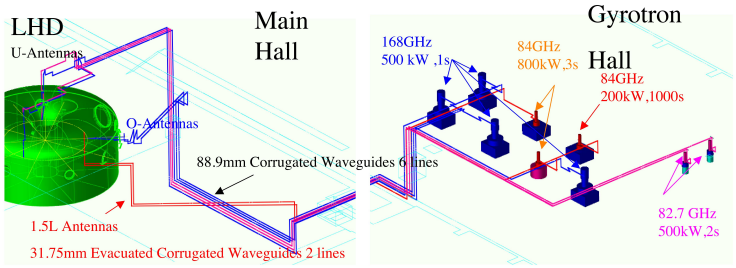

Fig. 1: *Bird eye's view of all ECRH system for LHD. 4-168 GHz, 2-84 GHz, 2-82.7 GHz gyrotrons are operated simultaneously. 6-88.9 mm, and 2-31.75 mm corrugated waveguide system transmit the power from gyrotron hall to the LHD. Both 31.75 waveguide system is evacuated and one of which is also used for long pulse experiment.*

two types of gyrotron power supply is used. One is for collector potential depression (CPD) type gyrotrons and the other is the conventional power supply for the non-CPD gyrotron. The others are for collector potential depression. These power supplies consist of three sets of collector power supply. Body and anode voltages are supplied independent inverter type power supplies. Two of the collector power supply is connected to triode type CPD gyrotrons (#1,2 ,3 and 7) at 168 GHz mainly used for the second harmonic heating. The other one is connected to the diode type CPD gyrotrons These combinations are listed in Table 1. Oversized non-evacuated corrugated waveguide with the diameter of 88.9 mm is introduced at first. Six lines of this type of transmission with total length of about 100 meters are in operational. From the beginning phase of the ECH system of LHD, we are suffered from arcing problems in the waveguides [6, 7]. The experience indicated that the threshold power of arcing increases as the purity of the HE_{11} excited in the waveguide. All MOU mirrors are optimized using the phase retrieval from the measurement output beam from each gyrotron. The accuracy of the alignment of the output beam from MOU to the waveguides is enhanced. In table 1 are also shown the power loss rate at the MOU and transmission efficiency for each line. It should be noted that the transmission efficiency for #11 and 12 are almost 90 %, although the number of miter bends and total path length are large. After this optimization, the threshold power for the arcing inside the waveguide appreciably increased. Relatively low efficiency for 168 GHz systems (#1-3,#7) and scatter of the values may be due to the sensitivity of the alignment of the input beam axis to that of waveguide. Low transmission efficiency for 31.75 mm diameter evacuated waveguides (#4 and 5) may be attributed to the low purity of the coupled HE_{11} mode. Since the axis alignment is less critical in the small diameter waveguide system, further optimization of the MOU mirrors or adjustment of the position of

Gyrotron No.	# 1	# 2	# 3	# 7	# 4	# 5	# 11	# 12
freq. (GHz)	168	168	168	168	84	84	82.7	82.7
manufacturer	Toshiba Triode	Toshiba Triode	Toshiba Triode	Toshiba Triode	Gycom Diode	Gycom Diode	Gycom Diode	Gycom Diode
spec. power (kW)	500	500	500	500	800	800	500	500
pulse width (s)	1	1	1	1	3	3	2	2
Power Supply	#1 CPD	#1 CPD	#1 CPD	#3 CPD	#2 CPD	#2 CPD	Non CPD	Non CPD
waveguide dia.(mm)	88.9 dry air	88.9 dry air	88.9 dry air	88.9 dry air	31.75 evacuated	31.75 evacuated	88.9 dry air	88.9 dry air
total length (m)	92	92	78	94	65	72	116	115
No. of Bends	18	21	16	21	10	10	19	15
Max. P_{in} (kW)	180	212	186	160	383	408	254	286
Max. width (s)	1.0	1.0	1.0	0.9	1.5	1.5	1.5	1.5
Loss at MOU (%)	23.0	24.0	14.0	32.8	10.0	10.0	8.5	6.5
Trans. Efficiency (%)	69.1	85.8	84.8	79.9	66.7	66.7	95.6	89.3

Table 1: *List of operated gyrotron and transmission lines in LHD*

the waveguide mouth might be necessary.

The power from each gyrotron is transmitted through a corrugated waveguide system and injected by a quasi-optical antenna system. Two sets of U (upper) port antenna consist of two sets of mirrors for 82.7 and 168 GHz. The antenna mirrors are designed using the phase constant method assuming Gaussian optics [8]. Designed beam waist sizes on the midplane of LHD are 15 and 50 mm in radial and toroidal direction. These values and its steerability on the midplane of the LHD are confirmed by low power test. Similar but symmetric and less focussed beams are formed in L (lower) and O (outer) ports. In each antenna system, final plasma facing mirror is plane mirror and can be steered by remote controlled super sonic motors around two axis (azimuth and elevation angle).

Due to the complexity of the configurations of the transmission system and quasi-optical antenna system, the setting of the antenna angles and polarizer rotation angles are not straightforward. Furthermore, the definition of the injection parameters on the frame of the LHD magnetic configuration is necessary and the actual quick selection and setting of these angles are required depending on the various experimental purposes. In order to perform effective local heating by the electron cyclotron waves, it is necessary to select more effective heating mode on the resonance among two eigen modes in the plasma. The desired polarization state to excite the effective mode is determined by the angle between injection and magnetic field directions at the interface of the injected beam to the plasma. The polarization state at the interface is controlled by the combination of rotation angles of two polarizers and antenna angles. Given the magnetic field configuration and the magnetic field strength, the optimum antenna setting angles can be

a) b)

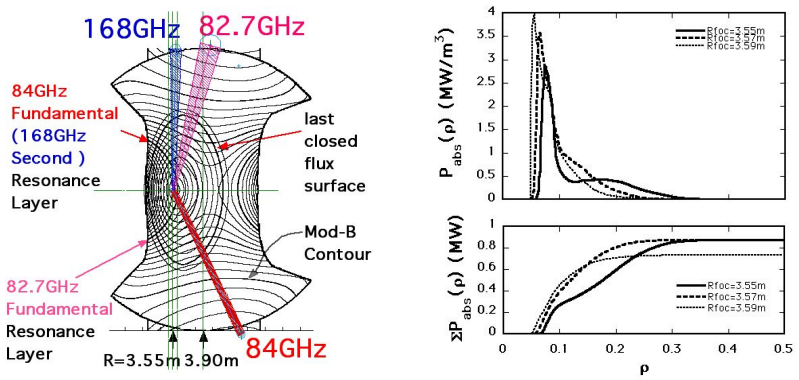

Fig. 2: *a) Flux surfaces and mod-B contours in LHD at vertically elongated cross section. Injected microwave beam from upper and lower antennas are shown with the beam waist size in scale. b)Expected power deposition profile calculated from ray tracing. Power from horizontal antenna is excluded in this calculation.*

determined using a geometrical configuration of the steering antenna. Once the injection angle of the beam is determined, the local magnetic field strength and the angle between injection and magnetic field direction at the interface of the plasma can be calculated. Using such derived magnetic field strength, the angle and the mode, the necessary polarization state can be calculated by the cold plasma dispersion relation. This polarization state is projected back to the polarizers to determine the best combination of the two polarizers.

Fig. 2 a) shows the injection beams, mod-B contours, and flux surfaces in the vertically elongated poloidal cross section. Two sets of upper beams, one lower beam from a vertical antenna, and two beams from horizontal antennas are used. In order to attain high electron temperature at center, the magnetic field strength and the confinement magnetic field configuration are selected to have a power deposition as nearly on axis as possible. One of the optimum combinations is the magnetic axis at 3.53 m and the toroidally averaged magnetic field strength on the axis at 2.951 T. The expected power deposition profile estimated by ray tracing, including the weakly relativistic effect [9,10], indicates that almost all of the injected power from the upper and lower antennas are concentrated within an averaged minor radius of $\rho \approx 0.2$ as shown in Fig. 2 b) , here, three cases of different injection angle is plotted to see the allowances and errors in antenna setting. Lower traces are integrated absorption power. Almost 100% power absorption can be expected in the density, and temperature regime discussed in this paper, provided that the beams crosses the resonance in the plasma confinement region. The injection po-

larization, so far is assumed to be pure X or O mode for the raytracing calculation. The injection polarization can also be controlled by setting a set of rotation angles of $\lambda/4$ and $\lambda/8$ plates installed in the waveguide transmission system. These setting angles for optimum focal point and polarization have been controlled independently using the remote control system.

Optimization of the Heating System

Square wave modulation experiments are performed at the averaged electron density of 1.0×10^{19} m^{-3} with flat profile, in order to get detailed power deposition profile when the focal position is scanned for 82.7 GHz and 168 GHz [13]. The boxcar technique is used for ± 3 ms data points at every turn on and off timings [3, 6] to deduce the first guess of the power deposition profile. The power deposition profile deduced from this method and that calculated from raytracing well coincides, especially in the case of fundamental resonance heating (82.7 GHz), although discrepancies in 168 GHz case are rather enhanced may be due to the limitation of the ray tracing calculation using geometrical optics. These results indicate that the control of focal point by steering mirrors work well as designed, but the deduction of power deposition using ECE data and calculation using geometrical optics needs more optimization [3].

The real polarization state at the far end of transmission line is checked by the newly developed polarization monitor described in the previous section. The results indicates that the the polarization state changes as designed. To check the polarization effect on the actual plasma heating, the angle α and also β is scanned for a constant target plasma, and to check total absorption power, or response of the central electron temperature. It is clarified that the optimum injection polarization is close to that expected polarization which excites X mode for second harmonic and O mode for fundamental heating near the plasma boundary ($\rho \approx 1$) or a little outer where the magnetic filed line is ergodic but low density plasma exist. Detailed study of the mode scrambling due to the shear [11] are left for the future work.

Attainment of T_{e0} = 10 keV and Formation of ITB

It had not been possible to do efficient heating by ECH on LHD due to the lack of the resonance condition on the axis. The magnetic field at the magnetic axis is increased by shifting the axis inward (R=3.5 - 3.6) from the standard position(R = 3.75 m) to locate the cyclotron layer across the axis. The injection beam aligned carefully, to hit the resonance on the magnetic axis. As a result, ECH beams were concentrated near the shifted axis. For the on axis heating, strongly focussed Gaussian beams at the fundamental and second harmonic resonances are directed to the resonances near the magnetic axis. The microwave sources used in this case were 84 GHz, two 82.7 GHz, and three 168 GHz gyrotrons. Fig. shows the injection beams, Mod-B contours, and flux surfaces in the vertically elongated

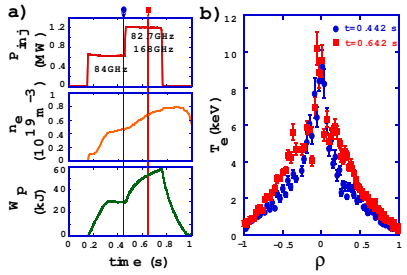

Fig. 3: *a)Time evolution of injected ECH power (upper), electron density (middle) and stored energy (bottom). b) T_e profile measured at each timing indicated by the arrow in a).*

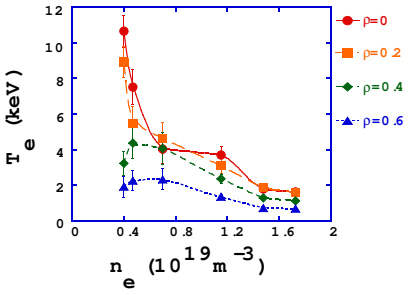

Fig. 4: *Dependence of T_e at ρ=0,0.2,0.4 and 0.6 on the electron density.*

poloidal cross section. Two sets of upper beams, one lower beam from a vertical antenna, and two beams from horizontal antennas are used. The magnetic field strength and the configuration are selected to have a power deposition as nearly on axis as possible. The selected magnetic axis is 3.53 m and the toroidally averaged magnetic field strength on the axis is 2.951 T. The expected power deposition profile estimated by ray tracing, including the weakly relativistic effect, indicates that almost all of the injected power from the upper and lower antennas are concentrated within an averaged minor radius of $\rho \approx 0.2$ as shown in Fig. 2 , here, three cases of different injection angle is plotted to see the allowances and errors in antenna setting. Lower traces are integrated absorption power. Almost 100% power absorption can be expected in the density, and temperature regime discussed in this paper, provided that the beams crosses the resonance in the plasma confinement region. Fig. 3 a) shows the evolution of plasma parameters and temperature profiles when the central electron T_{e0} exceeded 10 keV. The time evolution of the injected total power, the electron density, and the stored energy are shown here for the shot when the highest central electron temperature is recorded in the LHD. Almost 1.2 MW ECH power is concentrated inside $\rho \approx 0.2$. The electron density is slightly increasing but stays 0.5 to 0.6 $\times 10^{19}\mathrm{m}^{-3}$ in this case.

The two 84 GHz gyrotrons injected 0.7 MW to produce and heat the plasma. After the density and the stored energy had attained a quasi- steady state, the 168 GHz and 82.7 GHz power are added simultaneously. Although no additional gas puff is supplied, the density keeps increasing slightly. A high power YAG-Thomson scattering system is used at the times indicated by the arrows in Fig. 3 a). The profile is already sharp in the phase when only the 84 GHz power is injected. The 82.7 GHz power raises the central electron temperature to more than 10 keV. These high electron temperature modes appear only when the injected power exceeds a certain threshold level, and this threshold level increases with the

electron density. Figure 4 shows the dependence of the local electron temperaure at ρ = 0, 0.2, 0.4, and 0.6 on the averaged electron density under the same injection condition. Since the expected power deposition and the deposition profiles do not change significantly, the sharp increase in the electron temperature at ρ = 0, 0.2 suggests the presence of some non-linear mechanism. The feet of the ITB are more prominent when the ECH is applied on counter NBI target plasma. It is clear that the threshold power depends on the electron density. Other observations with respect to the ITB are: 1) The power deposition profile plays an important role in the formation of the ITB. The total deposited power inside $\rho < 0.2$ seems the key factor. 2) Reduction of the ion and impurity transport is in the ITB are suggested from impurity observations. formation indicates the presence of a positive electric field. 3) The location of the feet of the ITB depends on the direction of the NBI, which may be related to the position of the rational surface $\iota/2\pi$= 0.5 [12]. The $\iota/2\pi$ =0.5 surface plays an important role in expanding this interface outside. The clear ITB or foot point near ρ = 0.2 to 0.3 is observed in the case of counter NBI as a target plasma for ECRH. The slope of the temperature profile gradually increases and clear foot point disappears in the case of co-NBI. 4) The density and electron temperature region of electron root predicted from neoclassical theory coincides with the region where the ITB appears. These facts support the proposed anomalous transport reduction mechanism which the radial electric field shear reduces the fluctuation level and the shear itself is formed by the radial interface between electron and ion root [5]. The details of the formation of the ITB is under study using heat pulse propagation, here, the ITB is formed mainly by high power fundamental heating (84 and 82.7 GHz) and the modulated second harmonic heating is used as a perturbation source. The drastic difference in the transient transport between with and without ITB is observed. The time lag of the heat pulse propagation clearly changes across the ITB region. This analysis is also enabled by the optimization of the modulating 168 GHz injection system.

The forward and backward transition between ITB and normal confinement occurred when a part of the ECHRH power is the turned off and on to cross the threshold power for the ITB [4]. The decay time of the central temperature just after crossing down the threshold power is apparently long and high temperature gradient is kept for 60 ms. On the other hand, the decay time is short when the ECRH power kept below threshold. When the power increased stepwise crossing the threshold, high temperature gradient region grows gradually and the temperature profile jumps to form ITB about 40 ms after the stepwise increase. These results suggests that the temperature gradient helps to lower the threshold power for ITB formation [14].

Long Pulse Operation

Demonstration of steady state high Te plasma sustainment is important from the view point of extending the helical magnetic confinement device to the fusion reactor. Technical issue in the

CW ECH system is also important in the next step fusion device as ITER. Especially, the heat removal around gyrotron, MOU and transmission components are of critical issues. Development of low loss and safety component is required. Heat flux into the diverter and first wall Plasma density, temperature and particle control and sustainment in the steady state condition are to be established. A CW gyrotron with diamond window at the frequency of 84 GHz is introduced to perform the steady state plasma sustainment in LHD. This gyrotron is connected to one of the evacuated corrugated waveguide systems of 31.75 mm id. (#5) listed in Table. 1.

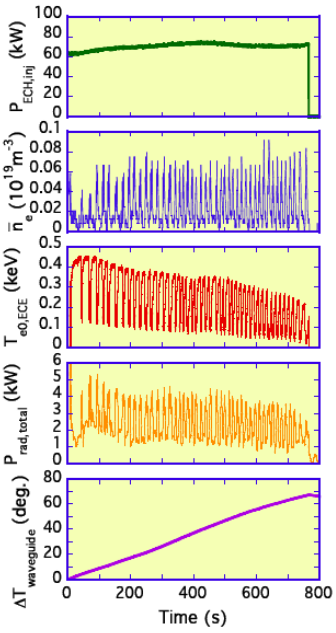

Fig. 5: *Time behavior of plasma parameters during 756 sec injection. a) Injected power, b) averaged electron density, c) ECE radiation temperature, d) Plasma radiation and b) temperature rise of a part of waveguide component, respectively*

In order to monitor the temperature rise in the waveguide components, multi-point temperature measurement system is introduced and attached the sensors along the long transmission line. Since,existing focusing antenna for this line had no cooling capability, a corrugated up taper from 31.75 mm id to 63.5 mm id is connected and the output beam is directed to a magnetic axis. Because of limited injection power, gas feed rate is controlled by repetitive pulse puff and its frequency. Almost all gyrotron parameters stayed almost constant during 766 sec injection. Collector, body voltages are well controlled and kept constant during the shot. Beam and body current and little increases with the time constant of 300 s and then saturates to be constant toward the end of the pulse. Temperature differences between inlet and outlet of the gyrotron coolant are still a little increasing even after such long pulse operation, but demonstrated that this gyrotron can be operated more than 1000 s with the power level at 150 kW. Pressure rise in MOU and waveguides due to the temperature rise had been the major cause of the termination of the pulse. Out gassing were far from saturation and the pressure kept increased due to the poor conductivity in the waveguide. Figure 5 show time evolutions of a) injection power, b) averaged electron density, c) ECE

radiation temperature, d) radiation power and e) temperature rise in waveguide component. The repetitive gas puff is controlled not to cause radiation collapse. This is the reason why the density, temperature, radiation fluctuates. In average, plasma of electron density of 2.4 $\times$ 10^{17} m^{-3}, and ECE radiation temperature of 240 eV (this is not necessarily the real electron temperature due optically thin) is sustained by 72 kW injection power. It is noted that the density decay rate just after the gas puffing pulse decreases towards the end of the pulse. This might reflect the change of recycling from the wall. It is necessary to continue the effort to increase the injection power by enforcing the cooling and pumping of the waveguide.

Conclusions

ECRH system have been upgraded step by step to inject total power more than 2 MW. The optimizations of the injection condition for almost all antennas are performed in the beam steering angle and also polarization. The power deposition profile is carefully controlled and utilized to achieve high electron temperature of more than 10 keV and formation of ITB. Sharp power deposition is also utilized in analyzing and understanding the transport mechanisms. Long pulse more than 12 minutes of 70 kW at 84 GHz is injected and sustained the plasma for 756 sec at the averaged density of 2.4 $\times$ 10^{17} m^{-3}.

References

[1] A. Iiyoshi, M. Fujiwara, O. Motojima *et al.* Fusion Technol. 17 (1990) 169.

[2] O. Motojima, H. Yamada, A. Komori *et al.* Phys. Plasmas 6 (1999) 1843.

[3] S. Kubo,*et al.* J. Plasma Fusion Res., 78 (2002) 99.

[4] T. Shimozuma, S. Kubo, H. Idei, Y. Yoshimura, *et al.* Plasma Physics and Controlled Fusion 45 (2003) 1183.

[5] A. Fujisawa, H. Iguchi, T. Minami, *et al.* Phys. Plasmas 7 (2000) 4152.

[6] S. Kubo , *et al* Proc. Radio Frequency Power in Plasmas. (1999) 485.

[7] T. Shimozuma, *et al* Fusion Engineering and Design,53 (2001) 525.

[8] S. Kubo,*et al.* Fusion Engineering and Design 26 (1995) 319.

[9] S. Kubo , *et al* Proc. 11th International Conf. on Plasma Phys. (2002),

[10] M. Bornatici , *et al* Nuclear Fusion, Vol. 23 (1983) 1153.

[11] H. Idei, *et al*, Fusion Engineering and Design, 53 (2001) 329.

[12] Y. Takeiri, T. Shimozuma, S. Kubo, *et al.* Phys. Plasmas 10 (2003) 1788.

[13] S. Kubo, H. Idei, T. Notake, *et al.* J. Plasma Fusion Research SERIES, Vol. 5 (2002) 584.

[14] M. Yokoyama, K. Ida, H. Sanuki, *et al.* Nucl. Fusion 42 (2002) 143.